Attracted diffusion-limited aggregation

S. H. Ebrahimnazhad Rahbari[1,2,*] and A. A. Saberi[3,4,†]

[1]*Plasma and Condensed Matter Computational Laboratory, Azarbayjan University of Tarbiat Moallam, Tabriz, Iran*
[2]*Department of Complex Fluids, Max-Planck Institute for Dynamics and Self-Organization, 37073 Göttingen, Germany*
[3]*Department of Physics, University of Tehran, Post Office Box 14395-547, Tehran, Iran*
[4]*Institut für Theoretische Physik, Universität zu Köln, Zülpicher Strasse 77, 50937 Köln, Germany*

In this paper we present results of extensive Monte Carlo simulations of diffusion-limited aggregation (DLA) with a seed placed on an attractive plane as a simple model in connection with the electrical double layers. We compute the fractal dimension of the aggregated patterns as a function of the attraction strength α. For the patterns grown in both two and three dimensions, the fractal dimension shows a significant dependence on the attraction strength for small values of α and approaches that of the ordinary two-dimensional (2D) DLA in the limit of large α. For the nonattracting case with $\alpha = 1$, our results in three dimensions reproduce the patterns of 3D ordinary DLA, while in two dimensions our model leads to the formation of a compact cluster with dimension 2. For intermediate α, the 3D clusters have a quasi-2D structure with a fractal dimension very close to that of the ordinary 2D DLA. This allows one to control the morphology of a growing cluster by tuning a single external parameter α.

I. INTRODUCTION

By immersing an object with a large surface-area-to-volume ratio into an ionic solution, it is surrounded by a double layer of electrical charge that significantly influences its surface behavior [1,2]. Electrical attraction of free ions with thermal motion in the fluid by the surface charge forms a second layer, known as the diffuse layer, that shields out the Coulomb potential of the surface layer and makes the whole structure electrically neutral. Applications of the double layer range from plasma physics [3] to colloidal science [4] and micro- and nanofluidics [5].

As a simple theoretical model for the formation of a diffuse layer in a special case, we implement extensive Monte Carlo simulations for attracted random walks (ARWs), introduced by Saberi [6], in order to study the formation of ionic aggregates on and near an infinite plane located at $z = 0$. An infinite surface charge exerts a uniform constant electric force on the free ionic particles in the fluid. It is therefore reasonable to consider an infinite attractive plane of uniform attraction strength α that acts on a free random walker launched from a point far from the attractive plane. An ionic *seed* is located at the center of the infinite plane. Upon contacting, the free ionic random walker sticks irreversibly to the cluster due to an absorbing bond introduced between the ionic particles.

The diffusion of an attracted Brownian particle of mass m in a fluid may be given by the Langevin equation

$$m\ddot{z} + \gamma\dot{z} + \alpha\,\mathrm{sgn}(z) = \xi(t), \tag{1}$$

where the second term denotes a viscouslike friction force with drag γ, the third term stands for an attraction force of strength α exerted by an infinite plane at $z = 0$, and $\xi(t)$ is a Gaussian white noise characterized by

$$\langle\xi(t)\rangle = 0, \quad \langle\xi(t)\xi(t')\rangle = 2D\delta(t - t'), \tag{2}$$

with D being the diffusion coefficient. We implement such a Langevin-like equation (1) to produce a diffusion-limited aggregated pattern on an attractive plane and investigate its fractal properties in terms of the strength of attraction α. We apply two different mechanisms in our model to produce the aggregates. First, the aggregates are allowed to grow freely in three dimensions, i.e., the three-dimensional (3D) ARW sticks to the aggregate upon touching the cluster giving rise to the formation of a 3D pattern. Second, the aggregates are restricted to grow only within the attractive plane, i.e., the 3D ARW sticks to the aggregate only if it touches the cluster within the attractive plane, which leads to the formation of a 2D pattern.

Our results indicate that for small α, the fractal dimensions for both cases depend significantly on the strength of attraction; in the limit of large α, they converge to the fractal dimension of the ordinary 2D diffusion-limited aggregation (DLA). This rapid convergence, however, implies the formation of a quasi-2D pattern for a 3D aggregate for intermediate values of α. Furthermore, for the two limiting cases, i.e., $\alpha = 1$ and $\alpha \to \infty$, our model reproduces the results of the ordinary DLA. Loosely speaking, for $\alpha = 1$, the 3D ARW is identical to the ordinary 3D random walk (RW) and thus our model generates the same patterns as the ordinary DLA in three dimensions. In the limit of $\alpha \to \infty$, the 3D ARW can move only within the attractive plane and is indeed identical to the 2D RW and thus, in both cases, the patterns of the ordinary DLA in two dimensions are reproduced. The only difference is for $\alpha = 1$ in two dimensions, where our model gives a different class of aggregates that are compact clusters with dimension 2.

The ordinary DLA, known also as a Brownian tree, was originally introduced by Witten and Sander [7] to model the aggregates of metal particles formed by adhesive contact in the low concentration limit. This model is shown to describe many pattern formation processes including dielectric breakdown [8], electrochemical deposition [9,10], viscous fingering, and Laplacian growth [11]. According to this model, the walker does a random-walk process initiated from infinity,

*sebrahi1@gwdg.de
†ab.saberi@ut.ac.ir

as described above in our model, but without experiencing any external force. Many of its fractal properties have then been reported from various simulations done both in real and mathematical planes (see, for example, Ref. [12] and references therein). This study uncovers insight into various related phenomena with a discrete time lattice walk [13,14], relaxation phenomena [15], exciton trapping [16], and diffusion-limited reactions [14,17].

II. ATTRACTED DIFFUSION-LIMITED AGGREGATION: DETAILS OF SIMULATION

In this section we investigate aggregation of ARWs on and near an attractive plane based on the algorithm proposed in Ref. [7] for ordinary DLA clusters, accompanied by the details of simulations. For M being the total number of particles, or equivalently the cluster *mass*, the simulation box is considered to be a cube of size $L_x = L_y = 20\sqrt{M}$ and $L_z = 60\sqrt{M}$. The box is divided into a regular lattice of $L_x \times L_y \times L_z$ cubic cells of unit size. Periodic boundary conditions are applied in all three directions. The attractive plane is a horizontal plane at $z = \frac{L_z}{2} \equiv 0$ whose bottom-left corner is taken as the origin of the coordinate system. We store information about each lattice site as an integer in the computer. Accordingly, the total memory to be occupied by the lattice will be equal to $4L_xL_yL_z \approx 10^5 M^{3/2}$ bytes. One can see that as the total number of particles M increases, the total memory grows rapidly and for large M the total memory becomes so huge that it cannot be handled by conventional computers. In order to prevent excessive memory usage, we apply different restrictions to our algorithm to reduce the memory. These tricks will be discussed separately for both 2D and 3D clusters in Secs. II A and II B, respectively.

First, let us briefly review the probabilities governing the movement of an ARW [6]. For the random walker at $z \neq 0$, there are six directions that can be chosen by the walker. One points towards the plane whose probability is set to αp, where $\alpha > 1$ is the strength of the attraction. For the other five directions, the corresponding probability of each link is equally set to p, providing $p = \frac{1}{\alpha+5}$. For the random walker at $z = 0$, there are two directions perpendicular to the plane whose probability is p' and four directions on the plane, each of which with the probability $\alpha p'$ such that $p' = \frac{1}{4\alpha+2}$. This setting of probabilities guarantees that the walker tends to ramble on and around the attractive plane.

It is well known that the formation of DLAs is dominated by diffusive motion rather than convective. Therefore, the walker must start moving far enough away from the attractive plane. Once a seed particle is settled on the attractive plane, a random walker is introduced on a random lateral position at height $z_0 = 15\sqrt{M}$ and moves according to the probabilities described above. The walker keeps moving until it sticks to the seed. Following that, a new random walker is introduced at $z_0 = 15\sqrt{M}$ from a random lateral position and is allowed to move until it sticks to one of those particles that are frozen. This procedure is applied until the desired number of particles in the cluster, i.e., M, is reached. For the growth of 2D and 3D structures, we implement different additional rules that will be discussed in Secs. II A and II B.

A. Two-dimensional structures

Two-dimensional structures are formed based on a landescape procedure. When a particle is at either $z = 1$ or -1, it may land on the plane if its shadow on the plane is not occupied; otherwise, it must escape to one of the five remaining directions with equal probability. Once the particle has landed on the plane, it will diffuse according to the aforementioned rules until it finds at least one frozen particle in its neighborhood and gets stuck to that point. It should be stressed out that according to the probabilities governing the motion of the ARWs, there still exists a probability for the walker to break from the plane and fly back into the space.

From our numerical experiments, we empirically found that the radial distance of the particles farthest from the seed never exceeds the $r = 8\sqrt{M}$ limit. We used this fact to accelerate our simulation runs in a way that the attractive plane is divided into two distinct regions: the inner region where the cluster forms and the outer region where the random walker moves freely with no need to explore a possible occupied nearest-neighbor site. We employed this fact in our simulations and found that it considerably decreases the computational effort.

In Fig. 1 two snapshots of the growing clusters on the attractive plane are shown for two different strength of attraction $\alpha = 1.2$ and 10 for the top and bottom figures, respectively. The cluster mass $M = 10^5$ and the distance from camera are considered to be the same for both patterns for a comparison.

FIG. 1. Snapshots of the growing clusters for $\alpha = 1.2$ (top) and $\alpha = 10$ (bottom) with the same number of particles $M = 10^5$. The radius of gyration is $R_G = 251.5$ and 410.54 for the top and bottom figures, respectively. The distance from camera is the same for both clusters. One can see that the gyration radius of the clusters R_G increases with the attraction strength α. Moreover, for the small α the cluster has fat arms, while for the larger α the chains are elongated and delicate. The pictures are rendered by the Pov-Ray software.
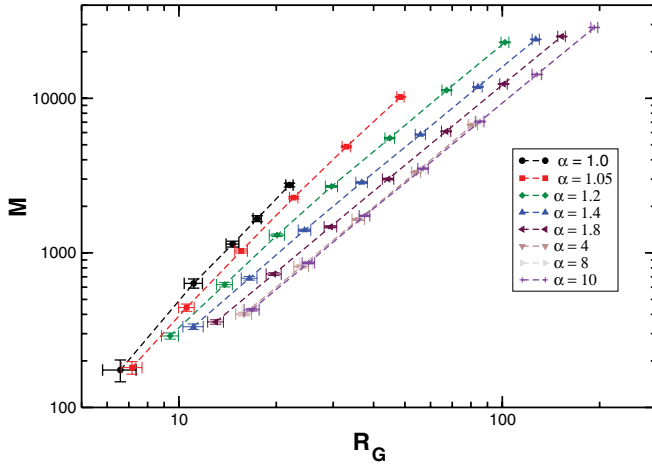
FIG. 2. (Color online) Cluster mass M as a function of the radius of gyration R_G of the 2D growing clusters on the attractive plane for different values of α. For $\alpha \gtrsim 1.15$, the curves exhibit a full power-law behavior Eq. (3).

Both figures have a fractal structure with a rotational symmetry about the z axis and the same number of main branches. For lower α, the particles are being condensed along the main arms, giving rise to much fatter branches than for the larger α, for which the cluster has delicate chains elongated on the attractive plane with deeper fjords and sharper tips. It is also evident that the gyration radius R_G of the clusters increases with the attraction strength α. Here the gyration radius (in units of a particle diameter) is found to be $R_G = 220.8$ and 410.54 for $\alpha = 1.2$ and 10, respectively.

In order to get a more quantitative insight into the structure of the clusters, we compute the gyration radius R_G of different clusters grown under the same conditions but with different strength of attraction α. Figure 2 illustrates the cluster mass M as a function of the gyration radius R_G of the clusters for various α. Since the ensemble averaging plays a crucial role in such computations, the averages for each point in Fig. 2 are taken over 90 different clusters for given values of α and M. It is well known that the following relation is usually held for fractal patterns:

$$M \propto R_G^{D_f}, \tag{3}$$

where D_f is the fractal dimension of the cluster. Our results are in accord with this power-law relation (3) for $\alpha \gtrsim 1.15$. For smaller values of α, the ARW crosses over to the ordinary 3D RW and starts to fill in the empty regions between the branches. This results in the cluster to being more condensed. A typical example of such a compact cluster for $\alpha = 1$ is shown in Fig. 3. Although the power-law behavior is disturbed, within our numerical accuracy, for $\alpha \to 1$, the cluster's outer perimeter may keep its fractal properties, as shown in Fig. 3.[1] A more detailed investigation of this is left for future work.

---

[1]This is similar to the compact islands appearing in a 2D cross section of a height profile in a $(2+1)$-dimensional Kardar-Parisi-Zhang equation [18].
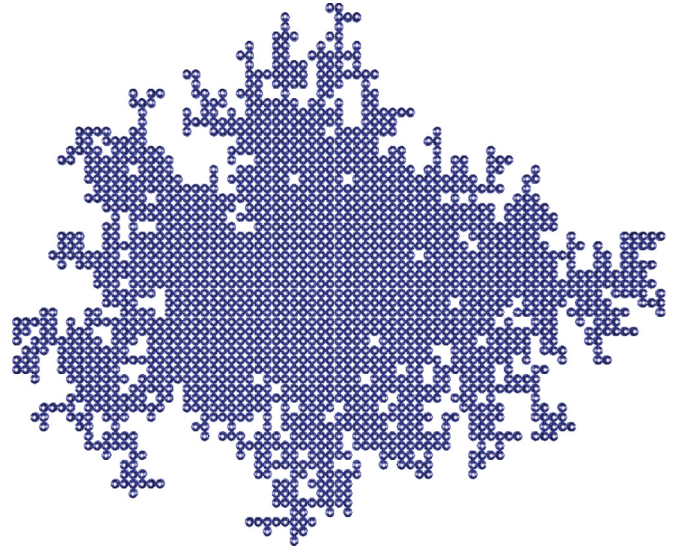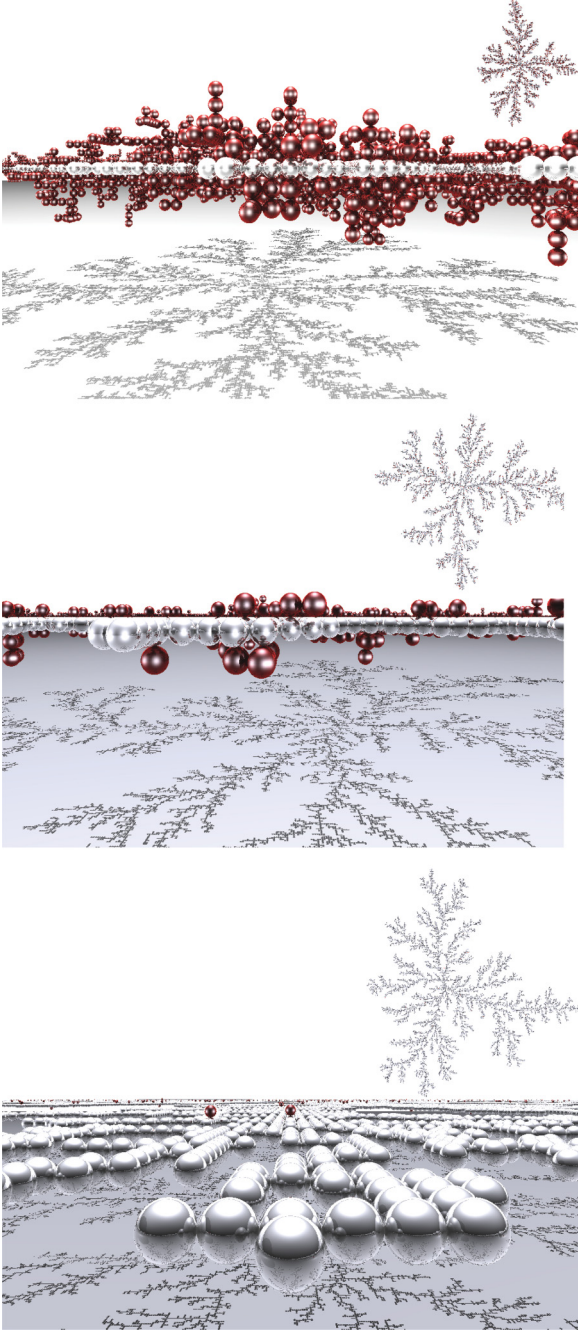

FIG. 3. (Color online) Typical example of a 2D cluster grown on the attractive plane with $\alpha = 1$. The number of particles is $M = 1875$, which forms a compact cluster of dimension ≈ 2, with gyration radius $R_G \simeq 19.62$.

According to our model, for $\alpha = 1$ the attraction strength is set to zero. As a principle of DLA, random walkers should initiate their motion from infinity (far from the seed). Therefore, there is a very little chance to find a random walker, triggered at infinity, on the surface of the attractive plane. Within this small chance, again there is a very little probability of keeping the particle moving on and around the plane. Once the particle lands on the plane, normally it tends to escapes to infinity and hardly finds a frozen particle in its neighborhood to join the cluster. Consequently, for 2D clusters at $\alpha = 1$ the growth rate is almost zero and we observe only clusters with small mass $500 < M < 3000$, which is not enough to examine any scaling relation. Therefore, we get poor statistics for $\alpha = 1$ (see also Fig. 6).

B. Three-dimensional structures

In contrast to 2D structures, the growth model for 3D clusters is not restricted to the surface of the attractive plane. Instead, the random walker in this case can get stuck in any lattice site with each of the nearest-neighbor sites already occupied, whether or not they are in the attractive plane.

In Fig. 4 we show some of the resulting patterns obtained by this algorithm in three dimensions. The figure shows a side view of the grown clusters consisting of $M = 10^5$ particles with $\alpha = 1.2, 2,$ and 10 with $R_G = 199.6, 342.8,$ and 405.9, from top to bottom, respectively. Two different colors are chosen for the particles: the metallic (light gray) color for those sitting on the attractive plane at $z = 0$ and red (dark gray) for particles sitting elsewhere with $z \neq 0$. As can be seen from the figure, the number of red (dark gray) particles is significantly dependent on the strength of attraction. For small α, the ARW can easily wander around and thus it is more likely for the particle to get a chance to stick to the cluster somewhere at $z \neq 0$; for larger α, the ARW is almost rambling on and near the attractive plane, which increases the sticking probability within the plane. In the limit of $\alpha \to \infty$,
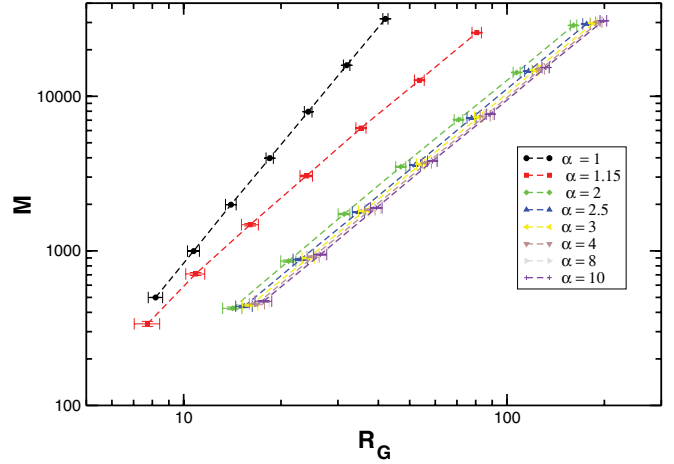
FIG. 5. (Color online) Cluster mass M as a function of the radius of gyration R_G of the 3D growing clusters formed around the seed placed on the attractive plane for different values of α.

FIG. 4. (Color online) Three typical examples of 3D grown clusters with a number of particles $M = 10^5$. The metallic (light gray) particles lie on the attractive plane and the rest, which are not on the surface, are illustrated by the red (dark gray). The strength of attraction is considered to be $\alpha = 1.2$, 2, and 10, with $R_G = 199.6$, 342.8, and 405.9, from top to bottom, respectively. The maximum height of the towers perpendicular to the attractive plane never exceeds a ten-particle diameter on either side of the attractive plane, implying the formation of quasi-2D clusters.

the 3D ARW falls onto the ordinary 2D RW, giving rise to the formation of ordinary DLA clusters in pure two dimensions. For $\alpha = 1$, at the other limiting side, the 3D ARW is the same as the ordinary 3D RW and we get back the ordinary 3D DLA patterns.

We empirically found that for $1 < \alpha < 1.2$, the thickness of 3D clusters on either side of the attractive plane never exceeds a 35-particle diameter, even for clusters of size up to $M = 10^5$. Also, for $\alpha > 1.2$, the height of the tallest tower in the cluster never reaches 10. Based on this experimental evidence, similar to that of the 2D case, the simulation box can technically be divided into two distinct volumes to reduce the memory: an inner volume, i.e., with $-35 \leqslant z \leqslant 35$ for $1 < \alpha < 1.2$ and $-10 \leqslant z \leqslant 10$ for $\alpha > 1.2$, where the cluster can form, and an outer volume where the particle moves freely without an extra check to look for an occupied nearest-neighbor site. We applied this fact in the structure of our programming codes and found that it considerably speeds up the simulations.

The quantity of interest is again the gyration radius R_G for clusters of different mass M. Figure 5 shows our results of cluster mass for 3D clusters as a function of their gyration radius for different attraction strength α. Each point in Fig. 5 is averaged over an ensemble of 90 independently grown samples. The mass of clusters is in the range $500 \leqslant M \leqslant 32\,000$. Error bars for both R_G and M are visible in the plot. We found a perfect scaling behavior for $\alpha \geqslant 2$, whereas for $1 < \alpha < 2$ our data fit a power law with higher uncertainty (this is also evident from the inset of Fig. 6). One can also see that for a constant cluster mass, the gyration radius increases upon increasing the attraction strength, which is due to the elongation of the growing cluster within the attractive plane. As mentioned above, the thickness d of the clusters along the z axis never exceeds a 70-particle diameter even for clusters of size up to $M = 10^5$. This implies a considerably small relative thickness, defined as $d/R_G \ll 1$, for the patterns and thus an indication of the formation of quasi-2D clusters. This will be confirmed in the following section, where we compute the fractal dimension of the grown patterns.

III. FRACTAL DIMENSION OF 2D AND 3D ADLA CLUSTERS

In this short section we compute the fractal dimension of the clusters as a measure characterizing the statistical complexity
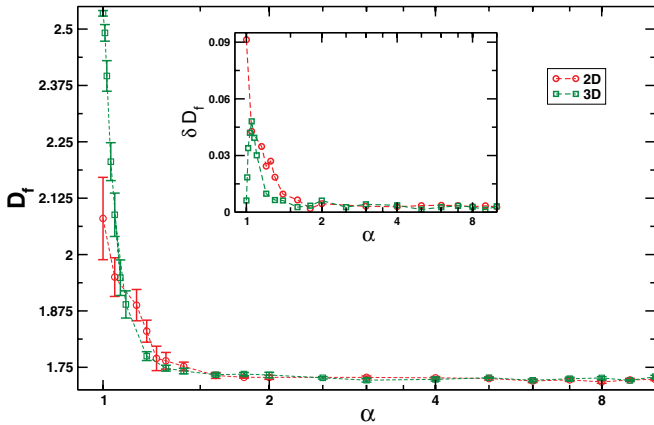
FIG. 6. (Color online) Fractal dimension D_f of the attracted diffusion-limited aggregation clusters grown in two and three dimensions, represented by open circles and squares, respectively, as a function of the attraction strength α. The inset shows the corresponding error bars within which the power-law behavior Eq. (3) holds.

of the grown fractal patterns in both two and three dimensions. The fractal dimension of the clusters can easily be calculated from the data given in Figs. 2 and 5 by examining the scaling relation (3).

In Fig. 6 we compile our data for the fractal dimensions of 2D and 3D clusters, which are represented by the open circles and squares, respectively. For both 2D and 3D clusters, the fractal dimension significantly depends on the strength of attraction α, especially for $\alpha < 2$. The smaller the α, the denser the clusters are. For larger α, the fractal dimensions in both cases are less dependent on α, rapidly converging to the value $D_f \approx 1.72$, which, within the statistical errors, is almost in accord with that of the ordinary DLA clusters in two dimensions with $D_f \approx 1.71$.

As discussed before, the overall intermediate fractal behavior seems to be dominated by the two crossover limits in the statistical behavior of the underlying diffusion process, i.e., the crossover of the 3D ARW to the ordinary 3D RW and 2D RW for $\alpha = 1$ and $\alpha \to \infty$, respectively. For $\alpha = 1$ the 2D clusters have a compact structure of dimension ≈ 2 and for the 3D clusters we obtain a fractal dimension $D_f \approx 2.53$ very close to the expected value for the ordinary 3D DLA [19].

IV. CONCLUSION

We introduced a model of aggregation based on an extension of diffusion-limited aggregation where the underlying diffusion process is a 3D Brownian motion (or a random walk on the lattice) that is attracted by a plane with strength α. The seed particle is placed on the attractive plane. In two dimensions, the fractal properties of the aggregated cluster are shown to be dependent on the attraction strength giving rise to the formation of patterns with $1.71 \lesssim D_f \leqslant 2$. The two limiting values for the fractal dimension D_f in the scaling region are discussed to be governed by the crossover of the 3D ARW to the ordinary 3D RW for $\alpha \to 1$ from one side

and its convergence to the ordinary 2D RW on the other side with $\alpha \to \infty$, which leads to ordinary 2D DLA patterns of $D_f \simeq 1.71$.

In three dimensions, the rotational symmetry, which is present in the ordinary 3D DLA clusters with $\alpha = 1$, is broken by the attractive plane with $\alpha > 1$ and the model leads to the formation of clusters with $1.71 \lesssim D_f \lesssim 2.53$. For intermediate α, we obtain quasi-2D clusters whose relative thickness, defined as the thickness of a cluster perpendicular to the attractive plane rescaled by its radius of gyration, is relatively small. Our results indicate a scaling region with $\alpha \gtrsim 2$, in which the fractal structure of the clusters can be characterized by a single fractal dimension $D_f \approx 1.72$, independent of α.

Recently, there has been growing attention and frequent reports on the fact that the morphology of self-assemblies can be controlled by tuning various physical parameters such as the packing fraction ϕ and the attraction strength. This is especially important for the handling of soft materials and food processing. In our study we found that a crossover from ramified, fractal clusters to compact aggregates occurs upon decreasing the attraction strength α at the limit of small attraction strength. For the two-dimensional clusters the threshold is found to be $\alpha_c = 1.15$. As a result, in our model the morphologies of the growing clusters can be controlled by tuning the attraction strength α.

In a recent study of aggregation of hard spheres [20], a similar crossover from a compact to ramified aggregation is found; in the former regime the scaling relation fails, while in the latter case the scaling holds. The crossover from compact to fractal clusters happens upon increasing the packing fraction ϕ. The threshold is found to be at $\phi = 0.55$, which is very close to the glass transition point at $\phi_g = 0.58$. Therefore, in this case, the structure of aggregations can be controlled by the packing fraction ϕ. Zhang *et al.* [21] report results of experiments on colloidal suspensions with short-range attraction and long-range repulsion. They show that the morphology of the clusters can be controlled by tuning either the attraction strength or the packing fraction ϕ resulting in an elongated-to-branched crossover.

These reports imply that the compact-to-ramified crossover may be considered a universal property of the aggregation of particles. Consequently, this suggests the possibility of proposing a single phase diagram that captures such behavior for different systems with different underlying physical processes and interparticle interactions.

Possible future work for constructing a much more realistic model of a diffusive layer may be an extension of the present model by considering a number of mobile seed particles on the attractive plane for which the growth of each can be given by our implemented procedure. In that case, the growing clusters can stick together upon contact.

[1] J. Lyklema, *Fundamentals of Interface and Colloid Science Vol. II: Solid-Liquid Interface* (Academic, London, 1995).

[2] R. J. Hunter, *Foundations of Colloid Science* (Oxford University Press, New York, 2001).

[3] N. A. Krall, *Principles of Plasma Physics*, 1st ed. (McGraw-Hill Inc., U.S., 1973).

[4] R. J. Hunter, *Foundations of Colloid Science*, 2nd ed. (Oxford University Press, 2000).

[5] B. J. Kirby, *Micro- and Nanoscale Fluid Mechanics: Transport in Microfluidic Devices* (Cambridge University Press, Cambridge, 2010).

[6] A. A. Saberi, Phys. Rev. E **84**, 021113 (2011).

[7] T. A. Witten Jr. and L. M. Sander, Phys. Rev. Lett. **47**, 1400 (1981).

[8] L. Niemeyer, L. Pietronero, and H. J. Wiesmann, Phys. Rev. Lett. **52**, 1033 (1984).

[9] R. M. Brady and R. C. Ball, Nature (London) **309**, 225 (1984).

[10] M. Matsushita, M. Sano, Y. Hayakawa, H. Honjo, and Y. Sawada, Phys. Rev. Lett. **53**, 286 (1984).

[11] L. Paterson, Phys. Rev. Lett. **52**, 1621 (1984).

[12] A. A. Saberi, J. Phys.: Condens. Matter **21**, 465106 (2009); F. Mohammadi, A. A. Saberi, and S. Rouhani, *ibid.* **21**, 375110 (2009); J. Phys. A **43**, 375208 (2010).

[13] J. Haus and K. W. Kehr, Phys. Rep. **150**, 263 (1987).

[14] A. Bunde and S. Havlin, *Fractal and Disordered Systems* (Springer, Berlin, 1991).

[15] C. A. Condat, Phys. Rev. A **41**, 3365 (1990).

[16] H. B. Rosenstock, Phys. Rev. **187**, 1166 (1969).

[17] G. H. Weiss and R. J. Rubin, Adv. Chem. Phys. **52**, 363 (1983).

[18] A. A. Saberi and S. Rouhani, Phys. Rev. E **79**, 036102 (2009).

[19] S. Tolman and P. Meakin, Phys. Rev. A **40**, 428 (1989).

[20] C. Valeriani, E. Sanz, P. N. Pusey, W. C. K. Poon, M. E. Catesb, and E. Zaccarellic, Soft Matter **10**, 1039 (2012).

[21] T. H. Zhang, J. Klok, R. Hans Tromp, J. Groenewold, and W. K. Kegel, Soft Matter **8**, 667 (2012).